ACS OMEGA

Open Access

http://pubs.acs.org/journal/acsodf

Article

Targeting Non-Apoptotic Pathways with the Cell Permeable TAT-Conjugated NOTCH1 RAM Fragment for Leukemia and Lymphoma Cells

Ryota Uchimura, Shinpei Nishimura, Mikako Ozaki, Manami Kurogi, Kohichi Kawahara, Masaki Makise, and Akihiko Kuniyasu*

Cite This: *ACS Omega* 2024, 9, 49925−49934

Read Online

ACCESS | Metrics & More | Article Recommendations | Supporting Information

ABSTRACT: Targeting nonapoptotic cell death offers a promising strategy for overcoming apoptosis resistance in cancer. In this study, we developed Tat-Ram13, a 25-mer peptide that fuses the NOTCH1 intracellular domain fragment RAM13 with a cell-penetrating HIV-1 TAT, for the treatment of T-cell acute lymphoblastic leukemia with aberrant NOTCH1 mutation. Tat-Ram13 significantly downregulated NOTCH1-target genes in T-ALL cell lines. Furthermore, the peptide had potent cytotoxic effects on various human leukemia and lymphoma cell lines. However, it did not affect normal lymphocytes and monocytes, some subsets of leukemia cells, or adherent tumor cells. This cell-selective cytotoxic activity was closely correlated with the peptide uptake via macropinocytosis in leukemia cells. In leukemia cells, Tat-Ram13 triggered rapid cell death. This cell death involved mitochondrial membrane depolarization and extracellular release of lactate dehydrogenase and high-mobility group box-1 protein without activation of caspase-3 or cleavage of PARP-1. These results suggest that Tat-Ram13 cell death is nonapoptotic and mediated by rapid plasma membrane rupture. Moreover, alanine scanning analysis identified four critical hydrophobic amino acids in the RAM13 domain essential for its cytotoxicity. Consequently, these results suggest that Tat-Ram13 is a tumor-selective, nonapoptotic cell death-inducing agent for treating refractory leukemia and lymphomas with apoptosis resistance.

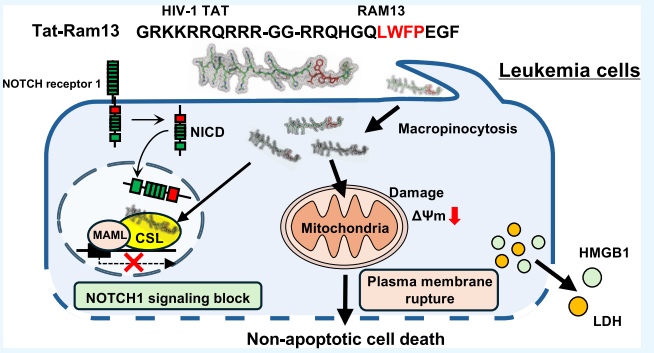

1. INTRODUCTION

T-cell acute lymphoblastic leukemia (T-ALL) is an aggressive hematologic malignant tumor characterized by the abnormal proliferation of immature thymocytes.[1,2] Despite improved survival rates in recent decades, treatment of relapsed and refractory T-ALL remains challenging, with a poor prognosis for patients unable to tolerate intensive chemotherapy.[3] Therefore, there is an urgent need to develop molecular-targeted therapies that are less cytotoxic and selective for T-ALL cells.

Notch receptors (NOTCH1−4) are transmembrane glycoproteins that regulate differentiation, proliferation, and survival.[4] Ligand binding to NOTCH triggers proteolytic processing, releasing the intracellular domain of NOTCH (NICD), which translocates to the nucleus. NICD forms a quaternary complex with DNA via the transcription factor CSL and the coactivator MAML, leading the transcription of NOTCH-dependent genes. A membrane-proximal RAM (RBP-jκ associated molecule) domain in NICD plays a critical role in facilitating the interaction between NOTCH and CSL. It binds specifically to the hydrophobic pocket of CSL through its ΦWΦP motif located at N-terminus of the RAM domain, ensuring the stability and functionality of the coactivator complex.[5]

Mutations in the *NOTCH1* gene, found in over 50% of T-ALL patients, lead to constitutively active forms of the NOTCH1, critical drivers of leukemia cell growth and metabolism.[6] These mutations cause the receptor to undergo ligand-independent cleavage, releasing the NICD, which acts as a transcription factor, activating cell proliferation and survival genes. Aberrant NOTCH1 signaling plays a critical role in T-ALL, making it a promising target for therapy.[4] γ-Secretase inhibitors (GSIs) have shown promising results in preclinical studies and are being studied as a potential treatment for NOTCH1-driven tumors.

Received: September 30, 2024
Revised: November 2, 2024
Accepted: November 14, 2024
Published: December 2, 2024

Many anticancer drugs induce apoptosis via caspase-mediated pathways, but defects in these pathways can result in drug resistance. Targeting nonapoptotic cell death mechanisms, such as ferroptosis, necroptosis, pyroptosis, and lysosome-dependent cell death, may offer therapeutic benefits in various tumor cells, especially in apoptosis-defective tumor cells, and help overcome chemotherapy resistance.[7,8] Despite these advances, many nonapoptotic cell death inducers lack tumor specificity, raising concerns about toxicity in normal tissues.

In this study, we developed a 25-mer antitumor peptide, Tat-Ram13, by fusing the RAM domain of the NOTCH1 intracellular fragment with the HIV-1 TAT peptide to directly antagonize NOTCH signaling in T-ALL. We examined its ability to inhibit NOTCH signaling using qPCR and observed its significant cytotoxic activity across various cancer cell lines, including leukemia and normal lymphoid cells. Furthermore, we explored the mechanism behind its cytotoxic effects and identified critical amino acids essential for this activity through alanine scanning of the Tat-Ram13 sequence.

2. RESULTS

2.1. Design and Synthesis of the Tat-Ram13 Peptide for NOTCH Signaling Inhibition. The 3D conformational information on the human NOTCH transcription factor ternary complex has allowed for the development of a peptide that inhibits NOTCH signaling.[9] The NOTCH intracellular domain (NICD) interacts strongly with the DNA binding protein CSL through its RAM domain (Figure 1A). The RAM domain contains a highly conserved hydrophobic tetrapeptide motif (Φ-Trp-Φ-Pro, where Φ represents a hydrophobic residue) near its *N*-terminus.[5] This motif is essential for binding to CSL in NOTCH signaling.

A previous study by Lubman et al. showed that a short peptide named RAM13, consisting of residues Arg^{1762}-Phe^{1774} in human NOTCH1, effectively disrupted interactions between NICD and CSL in human cell lysates.[10] This suggests that RAM13 could be a basis for developing peptide-based inhibitors targeting specific protein−protein interactions in NOTCH1 signaling. Expanding on this concept, we synthesized a cell-permeable RAM13 peptide, named Tat-Ram13, to inhibit NOTCH1 signaling in T-cell acute lymphoblastic leukemia (T-ALL) cells (Figure 1B,C). Tat-Ram13 is a fusion of the RAM13 peptide with a cationic, cell-penetrating HIV-1 TAT (48−57) peptide through a Gly-Gly linker. The WFP motif (Trp-Phe-Pro) is essential for binding the two proteins, and Ala substitution renders them incapable of binding.[10] We also generated an inactive mutant peptide, Tat-mRam13, in which all WFP motifs were replaced with alanine.

2.2. Inhibition of NOTCH1 Signaling Suppresses Cell Proliferation in Human T-ALL Cells. To assess the effects of Tat-Ram13 on transcriptional activity, we conducted qPCR analysis to examine the expression of three NOTCH target genes (*HES1*, *c-MYC*, and *NOTCH1*) in the NOTCH-dependent T-ALL cell line HPB-ALL. First, HPB-ALL cells were treated with the peptides, or the GSI compound DAPT, as a control for 16 h. When treated with 50 μM Tat-Ram13 and 30 μM DAPT, the expression of all three NOTCH target genes significantly decreased (Figure 2A). A mutant Tat-mRam13 (50 μM) did not affect the expression of *HES1* or *NOTCH1*, although it inhibits *c-MYC* expression. These data suggest that the Tat-Ram13 can inhibit NOTCH signaling by competitively inhibiting the interaction between CSL and NICD.

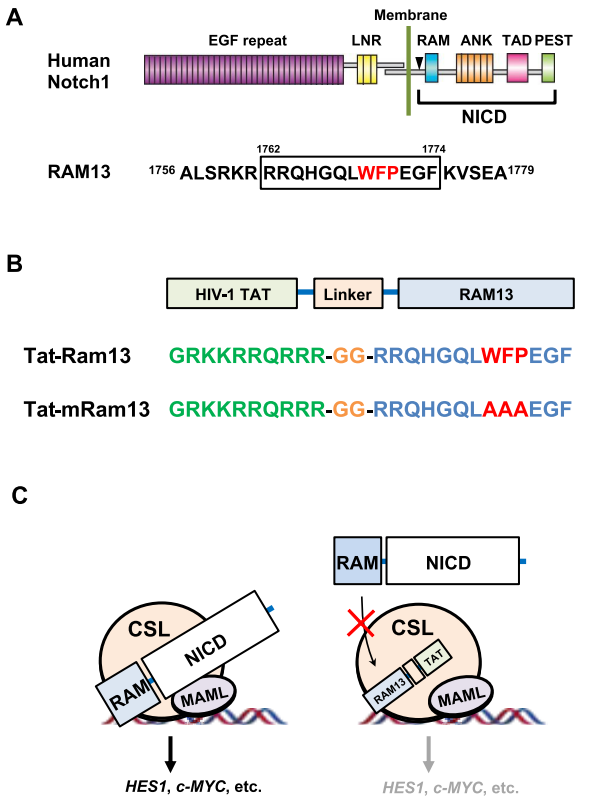

Figure 1. Strategy aims to block NOTCH signaling using a peptide analog. (A) The structure of human NOTCH1 and the RAM13 domain: The top diagram illustrates the domain organization of human NOTCH1, including EGF (epidermal growth factor) repeats, LNR (LIN-12/NOTCH repeats), TM (transmembrane domain), NLS (nuclear localization signal), RAM (RBP-jκ associated molecule), ANK (ankyrin repeat), and TAD (transactivation domain). An arrow indicates the γ-secretase cleavage site. The lower diagram shows the RAM13 peptide (in box), corresponding to residues 1762−1774 of human NOTCH1 protein. (B) The sequence of Tat-Ram13 and its mutant analog Tat-mRam13. Three essential amino acids (WFP) for NOTCH1-CSL interaction are highlighted in red. A Gly-Gly linker connects RAM13 or mutant RAM13 to the HIV-1 TAT (48−57). (C) The strategy of the direct inhibition of NOTCH1 signaling in T-ALL cells. Once internalized into the cell, the RAM13 domain of Tat-Ram13 competitively inhibits the interaction between NICD and CSL in the transcriptional complex in the nuclei. This inhibition suppresses cell proliferation and induce apoptosis by blocking the expression of NOTCH1 target genes, such as *c-MYC* or *HES1*.

Previous studies have shown that inhibition of NOTCH signaling induces cell-cycle arrest, apoptosis, and decreased proliferative capacity in a subset of T-ALL cell lines.[11] Therefore, we examined the growth inhibition effect of Tat-Ram13 on HPB-ALL cells (Figure 2B). GSI compound DAPT-treated HPB-ALL cells exhibited a significant reduction in proliferation, consistent with previously reported results.[12] Surprisingly, Tat-Ram13 reduced the total cell number more rapidly than DAPT, showing a more potent and rapid antiproliferative effect. Since the mutant Tat-mRam13 did not affect cell proliferation, Tat-Ram13 has a potent cytotoxic effect on T-ALL cells through a WFP motif-dependent mechanism.

https://doi.org/10.1021/acsomega.4c08955
ACS Omega 2024, 9, 49925−49934

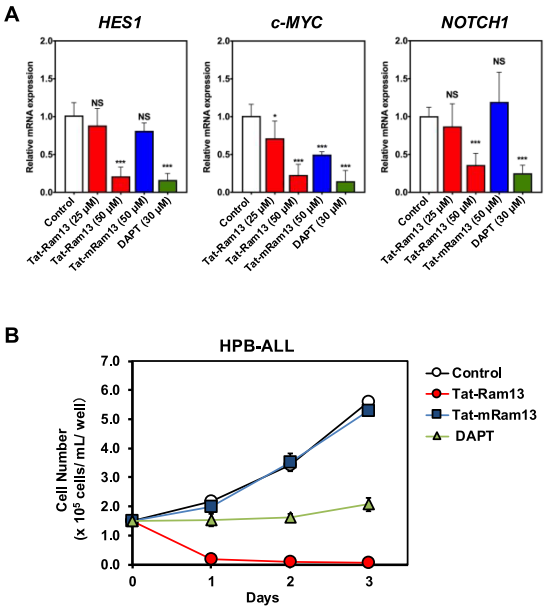

Figure 2. Effects of Tat-Ram13 on the NOTCH1 signaling pathway in human T-ALL cells. (A) Suppression of mRNA levels for NOTCH signaling target genes (*HES1, c-MYC, NOTCH1*) after 16 h of treatment with Tat-Ram13 (25 μM or 50 μM) and DAPT in human HPB-ALL cells. (B) Effects of Tat-Ram13 and DAPT on the proliferation of HPB-ALL cells. Cells were treated with either 15 μM DAPT (green triangles), 100 μM Tat-Ram13 (red circles), or 100 μM Tat-mRam13 (blue squares) or left untreated (control, open circles) and monitored for total cell count over 3 days.

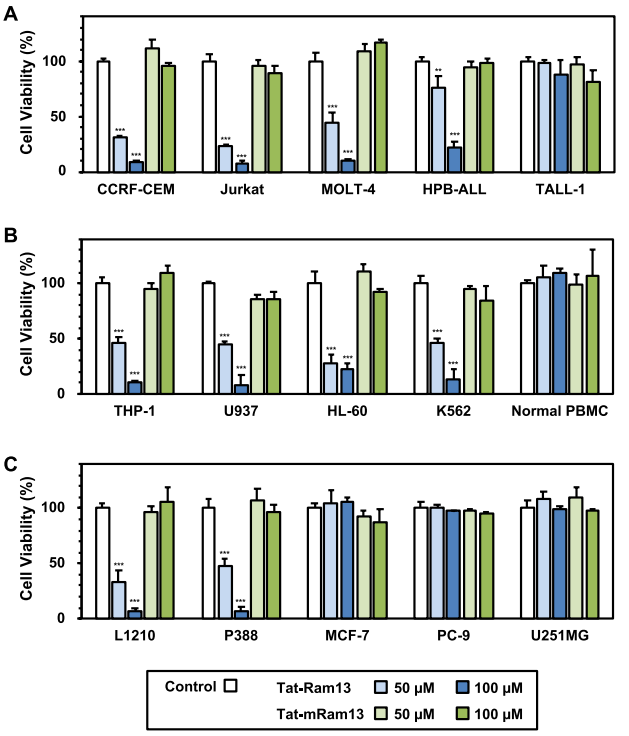

Figure 3. Effects of Tat-Ram13 peptide on the cell viability of various cells. (A) human T-ALL cell lines, (B) myeloid leukemia and lymphoma cell lines, and normal primary human mononuclear cells. (C) mouse leukemia and human adherent tumor cell lines. Cells were treated with or without Tat-Ram13 or Tat-mRam13 at indicated concentrations for 24 h. Cell viability was assessed using the WST-8 assay, with untreated cells (control) representing 100% viability.

2.3. Tat-Ram13 Exhibits Marked Cytotoxic Activity against Leukemia and Lymphoma Cells. We investigated the inhibitory effect of Tat-Ram13 on the proliferation of human and mouse leukemia and lymphoma cells, as well as normal human peripheral blood mononuclear cells (PBMC) comprising lymphocytes and monocytes, and various adherent cell lines. The cells were incubated with Tat-Ram13 or Tat-mRam13 for 24 h, and cell viability was measured. Figure 3A–C illustrates a dose-dependent decrease in cell viability of most leukemia and lymphoma cells following Tat-Ram13 treatment. Tat-mRam13 did not exhibit cytotoxicity in all these cell lines. In contrast, a human T-ALL cell line TALL-1 and normal PBMC were unaffected by Tat-Ram13. In addition, Tat-Ram13 did not affect the viability of three adherent cell lines (breast cancer cell MCF-7, lung carcinoma PC-9, and glioblastoma U251MG) at all (Figure 3C). Therefore, we also conducted cytotoxicity assays using concentrations greater than 100 μM on glioblastoma U-251MG cells. However, Tat-Ram13 did not affect cell viability in the cells (Figure S2A), although the internalization assay showed Tat-Ram13 entering the cells (Figure S2B). These results indicate that Tat-Ram13 demonstrates selective toxicity toward leukemia and lymphoma cells, but not normal lymphocytes and monocytes.

The cytotoxic action of this peptide may involve direct damage to the cell membrane. Hemolytic activity was measured using red blood cells in mice to investigate this possibility. The results show wed that Tat-Ram13 did not cause hemolysis even at a concentration of 150 μM (Figure S3). These findings suggest that the observed toxicity in leukemia cells is not caused by direct disruption of the cell membrane.

Interestingly, Tat-Ram13 significantly affects NOTCH-independent T-ALL cell lines (Figure 3A). Three T-ALL cell lines (CCRF-CEM, Jurkat, and MOLT-4), which carry activating *NOTCH1* mutations, are resistant to NOTCH inhibition due to PTEN loss.[12] In contrast, NOTCH-dependent, GSI-sensitive TALL-1 or HPB-ALL cell lines were less affected by Tat-Ram13 or required higher concentrations to induce cytotoxic effects than other Tat-Ram13-sensitive cell lines, respectively. Recent studies suggest that NOTCH signaling plays a tumor-suppressive role in AML, and inhibiting NOTCH signaling enhances the proliferation of AML cell lines.[13] As shown in Figure 3B, Tat-Ram13 exhibited cytotoxicity against all tested AML cell lines (THP-1, HL-60, U937). In addition, K562, an erythroleukemia cell line that proliferates via a BCR-ABL-driven pathway not dependent on NOTCH signaling, underwent cell death after treatment with Tat-Ram13. These results conclude that Tat-Ram13-induced cytotoxicity is not dependent on NOTCH signaling inhibition despite its ability to downregulate NOTCH1 target genes.

2.4. Cell-selectivity of Tat-Ram13 is Associated with Macropinocytic Activity in Leukemia Cells. Tat-Ram13 markedly reduced cell viability in most human leukemia and lymphoma cells but did not affect TALL-1 cells or normal PBMC (Figure 3A,B). To understand the mechanism underlying the differences in cell-selective cytotoxicity, we examined whether Tat-Ram13 is taken up by the target cells using the fluorescent-labeled probe Tamra-Tat-Ram13. Confocal fluorescence microscopy revealed that Tamra-Tat-Ram13 was significantly taken up by Tat-Ram13-sensitive CCRF-CEM and Jurkat cells (Figure 4A). In contrast, TALL-1 cells and

https://doi.org/10.1021/acsomega.4c08955
ACS Omega 2024, 9, 49925−49934

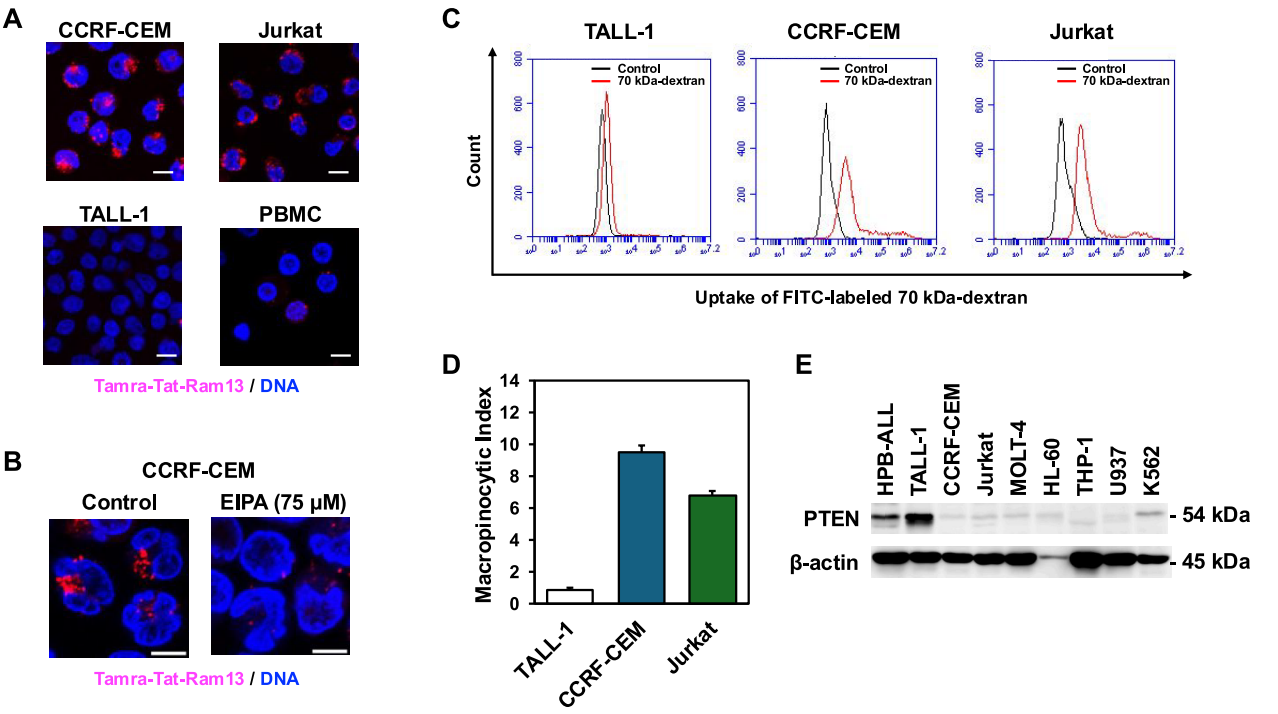

Figure 4. Cytotoxicity of the Tat-Ram13 is correlated with the macropinocytic activity of the T-ALL cells. (A) Intracellular uptake of fluorescent-labeled Tamra-Tat-Ram13. Human T-ALL cells and human primary peripheral blood mononuclear cell (PMBC) were incubated with 3 μM of fluorescent-labeled Tamra-Tat-Ram13 (red) for 30 min, and subsequently observed by confocal fluorescent microscopy. The scale bar indicated 10 μm. (B) Effect of macropinocytosis inhibitor EIPA on the uptake of Tamra-Tat-Ram13 in CCRF-CEM cells. (C) Measurement of macropinocytic activity of T-ALL cell lines. Cells were incubated with fluorescent probe FITC-labeled 70 kDa-dextran for 30 min, and the intracellular uptake was analyzed by flow cytometry. A flow cytometry histogram plot illustrates the uptake of 70 kDa-dextran (red line) in comparison to the control (black line). (D) The macropinocytic index in three T-ALL cells. The levels of macropinocytic activity were determined by flow cytometric analysis. The values for both CCRF-CEM and Jurkat cells were normalized to 1.0 based on the uptake in TALL-1 cells. (E) Western blot analysis of protein expression of PTEN in various human leukemia cells.

normal PBMCs, which are insensitive to Tat-Ram13, showed negligible intracellular uptake of Tamra-Tat-Ram13. These results indicate that the cytotoxicity of Tat-Ram13 is closely associated with its cellular uptake.

Basic cell-penetrating peptides, such as HIV-1 TAT and octa-arginine (R8), are reported to enter cells primarily through macropinocytosis.[14,15] Macropinocytosis has been observed in a variety of cancer cells, yet we have shown that leukemia and lymphoma cells undergo macropinocytosis using a leukemia cell-selective cyclic peptide.[16] Therefore, we investigated the effect of a macropinocytosis inhibitor on CCRF-CEM cells to determine whether the uptake of Tamra-Tat-Ram13 is mediated by macropinocytosis (Figure 4B).

The cells were pretreated with 5-(*N*-ethyl-*N*-isopropyl)-amiloride (EIPA), a known macropinocytosis inhibitor,[17] for 90 min. As a result, this pretreatment led to a significant decrease in the fluorescent signal of Tamra-Tat-Ram13. These findings strongly suggest that macropinocytosis plays a major role in the uptake of Tamra-Tat-Ram13 in leukemia cells. Furthermore, we measured the macropinocytic activity of each cell type and compared it with the cytotoxicity of Tat-Ram13. In our assessment, we used a fluorescein probe FITC-labeled 70 kDa-dextran (70 kDa-Dex), a widely utilized marker for macropinocytosis.[17] Flow cytometric analysis revealed that CCRF-CEM and Jurkat cells exhibited significantly higher uptake of 70 kDa-Dex compared to TALL-1 cells (Figure 4C). The macropinocytic index values of CCRF-CEM and Jurkat are 9.5- or 6.8-fold higher than those of TALL-1, respectively (Figure 4D). These data suggest that cellular uptake of Tat-Ram13 correlates with macropinocytic activity, reflecting differences in Tat-Ram13 cytotoxicity among the leukemia cells.

Macropinocytosis is regulated via Rac-Pak signaling activation by phosphoinositide 3-kinase (PI3K).[18] Phosphatase and tensin homologue deleted on chromosome 10 (PTEN) is as the tumor suppressor gene for its negative regulation of the phosphatidylinositol 3-kinase (PI3K) pathway. Recent reports demonstrated that *PTEN*-deficient tumor cells show high macropinocytic activity for survival.[19−21] Therefore, we analyzed the levels of PTEN protein expression in human leukemia and lymphoma cell lines used. Western blot analysis showed that cell lines susceptible to Tat-Ram13-induced cell death exhibited little or no PTEN expression (Figure 4E). In contrast, TALL-1 cells, resistant to Tat-Ram13, and HPB-ALL cells, which displayed low sensitivity to Tat-Ram13, showed normal levels of PTEN protein expression. These findings suggest that the cytotoxic activity of Tat-Ram13 is negatively correlated with PTEN protein expression levels, indicating that Tat-Ram13 is more effective against *PTEN*-deficient or low-PTEN leukemia/lymphoma cells in a macropinocytosis-dependent manner.

2.5. Tat-Ram13-Induced Nonapoptotic and Lytic Cell Death in Leukemia Cells. Our data suggest that Tat-Ram13-elicited cytotoxicity is not caused by inhibition of NOTCH signaling (Figure 3A−C). Using CCRF-CEM cells, we determined the mode of cell death induced by Tat-Ram13 and compared it to apoptosis induced by the DNA topoisomerase II inhibitor etoposide. First, we investigated

https://doi.org/10.1021/acsomega.4c08955
ACS Omega 2024, 9, 49925−49934

the time course of cell death in Tat-Ram13- and etoposide-treated CCRF-CEM cells (Figure 5A). At 100 μM of Tat-

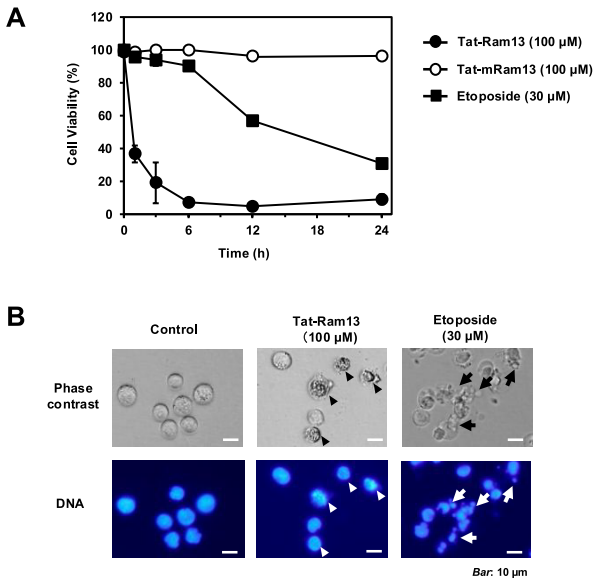

Figure 5. Tat-Ram13 induces cell death distinct from etoposide-induced apoptosis. (A) The time course of cell death induced by Tat-Ram13 or etoposide in CCRF-CEM cells. Cells were treated with Tat-Ram13, Tat-mRam13, or etoposide for 24 h at the indicated concentrations. Cell viability was then determined using a trypan blue exclusion assay. (B) Phase-contrast and DNA images of CCRF-CEM cells treated with Tat-Ram13 (100 μM) or etoposide (30 μM) for 24 h. Scale bars in the images represent 10 μm. Swelling cells with shrunken nuclei are indicated by arrowheads, and arrows indicate DNA fragmentation.

Ram13, cell viability decreased to less than 30% within 0.5 h in CCRF-CEM cells, whereas etoposide-induced cell death occurred more slowly. These data show that cells treated with Tat-Ram13 undergo rapid cell death, indicating that this phenomenon is not due to the suppression of cell proliferation through NOTCH signaling.

Second, we observed cell morphology by microscopy after treating CCRF-CEM cells with Tat-Ram13 for 24 h (Figure 5B). When exposed to etoposide, we observed characteristic signs of apoptosis such as membrane blebbing and DNA fragmentation. However, cells treated with Tat-Ram13 did not exhibit these features. Instead, these cells displayed cell swelling and nuclear shrinkage, suggesting that cell death induced by Tat-Ram13 is distinct from apoptotic cell death.

To evaluate whether Tat-Ram13 induces apoptosis in CCRF-CEM cells, we investigated the activation of caspase-3, a critical executioner of apoptosis, and the cleavage of its substrate PARP-1, in comparison to the apoptosis-inducing agent etoposide. Western blot analysis revealed that Tat-Ram13 did not induce caspase-3 cleavage in CCRF-CEM cells, unlike etoposide, which did produce the cleaved fragment, indicating caspase-3 activation (Figure 6A). Similarly, Tat-Ram13 did not lead to the cleavage of PARP-1 fragments (89 kDa) as etoposide did. This result suggests that Tat-Ram13 does not activate caspase-3 during cell death.

To further confirm the lack of caspase activation in Tat-Ram13-treated CCRF-CEM cells, we pretreated the cells with a pan-caspase inhibitor, z-VAD-fmk. Pretreatment with z-VAD-fmk did not affect the cell death rate in Tat-Ram13-treated

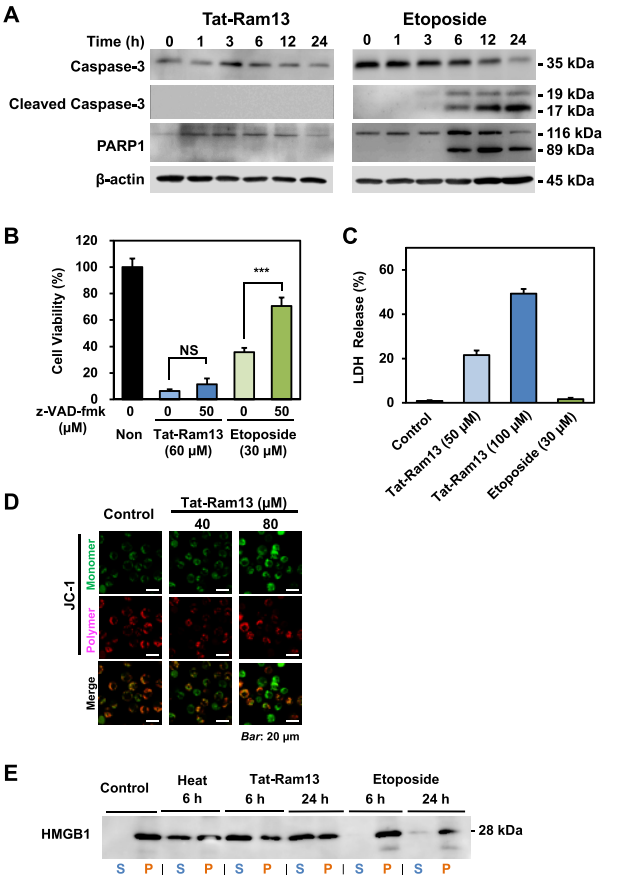

Figure 6. Tat-Ram13 induces nonapoptotic cell death in leukemia cells. (A) Western blot analysis of caspase-3 and PARP1 cleavage in CCRF-CEM cells treated with 100 μM Tat-Ram13 or 30 μM etoposide. (B) Effect of the caspase inhibitor z-VAD-fmk on the cytotoxicity of Tat-Ram13 (60 μM) or etoposide (30 μM) in CCRF-CEM cells. Cells were preincubated with or without 50 μM z-VAD-fmk for 45 min, and cell viability was measured by WST-8 assay. (C) Confocal images of mitochondrial membrane depolarization in Tat-Ram13-treated CCRF-CEM cells. An increased green/red ratio of JC-1 dye indicates membrane depolarization. (D) Lactate dehydrogenase (LDH) release from CCRF-CEM cells treated with Tat-Ram13 and etoposide for 3 h. (E) Detection of HMGB1 protein released from dead cells. Supernatants containing extracellularly released HMGB1 (S) and cell pellets containing unreleased HMGB1 (P) were detected by Western blotting analysis.

CCRF-CEM cells (Figure 6B), whereas it significantly reduced the cell death rate in etoposide-treated cells. These data indicate that caspase activation is not involved in the cell death mechanism induced by Tat-Ram13, suggesting that the mode of Tat-Ram13-induced cell death is nonapoptotic.

Since caspase activation did not occur during Tat-Ram13-induced cell death, we investigated whether changes in mitochondrial membrane potential were responsible. We used the fluorescent dye JC-1, which shifts from green to red emission in response to changes in membrane potential, to assess mitochondrial depolarization.[22] Confocal microscopy observation revealed that the Tat-Ram13 treatment increased the green/red fluorescence ratio of JC-1, signifying enhanced mitochondrial depolarization (Figure 6C). Despite the absence of caspase-3 activation, these results suggest that Tat-Ram13-induced cell death significantly reduces mitochondrial membrane potential.

https://doi.org/10.1021/acsomega.4c08955
ACS Omega 2024, 9, 49925−49934

Nonapoptotic cell death mechanisms, such as pyroptosis, necroptosis, ferroptosis, NETosis, and lysosome-dependent cell death, often lead to plasma membrane rupture and the release of inflammatory molecules.[23] We measured two marker proteins for plasma membrane rupture: lactate dehydrogenase (LDH) and high mobility group box 1 (HMGB1). As shown in Figure 6D, Tat-Ram13-treated cells released significant amounts of LDH into the cell culture supernatant within 3 h of treatment, while etoposide-treated cells did not. These findings suggest that Tat-Ram13 treatment leads to rapid plasma membrane rupture. Western blot analysis found that CCRF-CEM cells exposed to Tat-Ram13 released high levels of HMGB1 into the culture supernatant, the same as those found in heat-treated necrotic cells (Figure 6E). Conversely, cells treated with etoposide for 24 h released very little HMGB1, with most remaining in the dead cells.

We also investigated the cell death process induced by Tat-Ram13 using various cell death inhibitors, including necrostatin-1 for necroptosis, ferrostatin-1 for ferroptosis, disulfiram for pyroptosis, and pepstatin A and E-64d for lysosome-dependent cell death. None of the inhibitors tested prevented the reduction in cell viability induced by Tat-Ram13 (data not shown).

2.6. Identification of Essential Amino Acids in the Ram13 Sequence Necessary for its Cytotoxic Activity. We conducted an alanine scanning analysis to identify critical amino acids in the Ram13 sequence responsible for its cytotoxicity (Figure 7A). Our cytotoxicity assays confirmed that the WFP motif is crucial, as the mutant Tat-mRam13 was ineffective. We focused on the residues surrounding the WFP motif and synthesized seven mutant peptides, each with a single alanine substitution in the RAM13 sequence. Treatment of CCRF-CEM cells for 24 h resulted in a complete loss of cytotoxic activity for the Trp substitution and partial reduction for the Leu, Phe, and Pro replacements. These data indicate that these four hydrophobic amino acids are crucial for the cytotoxicity of Tat-Ram13. Interestingly, these critical residues are identical to the ΦWΦP motif, including WFP, and are essential for interacting with the NOTCH1 and CSL proteins.[10]

Next, we explored the role of the cell-penetrating part by replacing the HIV-1 TAT sequence with octa-arginine (R8). As shown in Figure 7B, R8-Ram13 showed significantly higher cytotoxicity than Tat-Ram13, while R8-mRam13 remained inactive, confirming the necessity of a functional cell-penetrating sequence. Ram13 alone, without the cell-penetrating domain, lost its cytotoxicity.

Basic cell-penetrating peptides such as HIV-1 TAT and R8 interact with negatively charged heparan sulfate proteoglycans (HSPGs) for cellular entry.[14,15] Therefore, we assessed the cytotoxicity of Tat-Ram13 in the presence of heparin, a competitor of HSPG with negatively charged polysaccharides (Figure 7C). The results showed that heparin completely restored the cell viability in a dose-dependent manner. This suggests that the positive charge of the Tat domain is crucial for binding and internalization.

In summary, the Tat-Ram13 sequence structure relies on the essential intracellular uptake of the negatively charged residues of the TAT domain and the cytotoxic activity of four hydrophobic amino acids of the RAM13 domain.

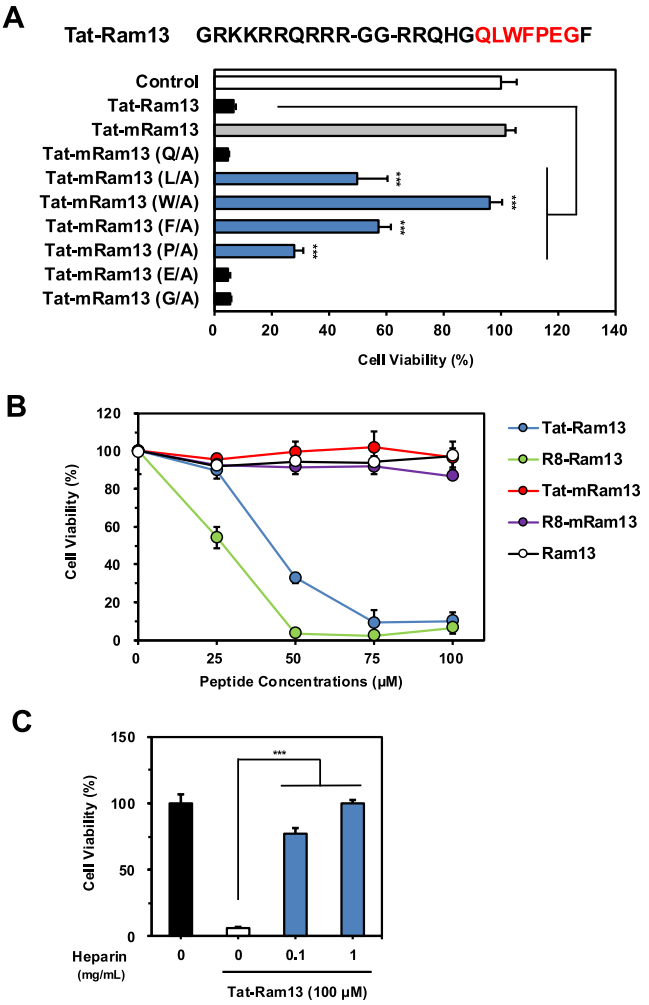

Figure 7. Relationship between structure and cytotoxicity in Tat-Ram13. (A) Four hydrophobic amino acids (L, W, F, and P) in RAM13 domain are crucial for the cytotoxicity of 100 μM Tat-Ram13. Substituting these amino acids with alanine significantly reduced cytotoxicity in CCRF-CEM cells. In the Tat-Ram13 sequence, seven Tat-mRam13 mutants had the amino acids highlighted in red replaced with alanine. (B) The cell-penetrating TAT motif can be substituted with an octa-arginine (R8) sequence. R8-Ram13 showed more significant cytotoxic activity in CCRF-CEM cells compared to Tat-Ram13. Two mutant RAM13 peptides (Tat-mRam13 and R8-mRam13) and Ram13, which lacks a cell-penetrating domain, are inactive. (C) Positively charged amino acids in the TAT motif are vital for cytotoxicity. The cytotoxicity of Tat-Ram13 (100 μM) decreased in the presence of 0.1 or 1.0 mg/mL of heparin.

3. DISCUSSION

In this study, we developed a 25-mer fusion peptide, Tat-Ram13, by combining the NOTCH1 intracellular domain fragment RAM13 with the HIV-1 TAT peptide. Tat-Ram13 shows potent cytotoxic effects on various leukemia and lymphoma cell lines, enhancing macropinocytic activity while not damaging normal peripheral blood cells. Furthermore, Tat-Ram13 triggers nonapoptotic cell death through mitochondrial membrane depolarization and plasma membrane disruption, releasing inflammatory molecules.

The present study addressed the correlation between *PTEN*-deficiency and increased macropinocytic activity in leukemia cells (Figure 4B,C). PTEN loss hyperactivates the PI3K

https://doi.org/10.1021/acsomega.4c08955
ACS Omega 2024, 9, 49925−49934

pathway, a key regulator of macropinocytosis.[18] Recent studies have demonstrated that *PTEN*-deficiency enhances macropinocytic activity in various cancer cells.[20,21,24] Tat-Ram13 could target this endocytic pathway in *PTEN*-deficient leukemia cells, suggesting its potential as a tumor-selective therapy. In the present study, even at high concentrations (>150 μM), Tat-Ram13 does not kill adherent tumor cell lines (Figure 3C). Generally, aggressive adherent cells exhibit high macropinocytic activity.[24] We showed the efficient uptake of Tat-Ram13 in aggressive glioblastoma cells (Figure S3). The difference in Tat-Ram13 cytotoxicity between adherent and leukemia cells may be attributed to distinct intracellular trafficking or processing of Tat-Ram13 after its uptake, affecting its ability to induce cell death. However, the precise mechanism underlying the involvement of macropinocytosis in Tat-Ram13 cytotoxicity remains unclear and requires further investigation, particularly regarding its uptake mechanisms across different cell types.

The anticancer properties of Tat-Ram13 set it apart from other NOTCH inhibitors. A successful peptidic NOTCH inhibitor, SAHM1, primarily inhibits NOTCH-dependent pathways, similar to the action of GSIs.[25] While SAHM1 effectively suppresses the proliferation of GSI-sensitive T-ALL cell lines, it shows no significant effect on GSI-insensitive, NOTCH-independent cells.[25] Conversely, Tat-Ram13 has a broader range of cytotoxic effects, including significant activity against NOTCH-independent leukemia and lymphoma cells. Although the precise mechanism by which Tat-Ram13 induces nonapoptotic cell death remains unclear, these findings suggest that mechanism of action of Tat-Ram13 extends beyond canonical NOTCH inhibition.[5]

Nonapoptotic cell death mechanisms such as necroptosis, pyroptosis, and ferroptosis offer potential therapeutic avenues in apoptosis-resistant tumors, potentially strengthening the effectiveness of immunotherapy.[7,26,27] However, current inducers of nonapoptotic cell death, such as RSL3 for ferroptosis, lack tumor specificity.[28,29] Tat-Ram13 presents a promising alternative by targeting malignant cells while minimizing normal tissue toxicity, thus crucially reducing adverse effects.

Recent studies have discovered "oncolytic peptides" that selectively induce nonapoptotic cell death in cancer cells.[30−32] Tat-Ram13 triggers fundamental cell death processes, including mitochondrial membrane depolarization and plasma membrane rupture. While Tat-Ram13 shares membrane-disrupting properties with other oncolytic peptides, its unique structural features, such as its basic cell-penetrating domain and hydrophobic residues (L−W−F-P), likely contribute to its specific selectivity toward cancer cells. Despite the lack of sequence homology, these peptides may act through a common, yet unidentified, functional pathway. Further research is required to elucidate how Tat-Ram13 and other oncolytic peptides exert their selective cytotoxic effects, particularly outside of well-known pathways like necroptosis and ferroptosis. This could potentially unveil novel non-apoptotic cell death mechanisms and new molecular targets for cancer therapies beyond CSL proteins associated with NOTCH1 signaling.

4. CONCLUSIONS

This study shows that Tat-Ram13 induces potent, tumor-selective cytotoxicity in leukemia and lymphoma cells, while also blocking NOTCH1 signaling. Notably, Tat-Ram13 triggers nonapoptotic cell death in PTEN-deficient leukemia cells with high macropinocytic activity, revealing a distinct mechanism of action. These results suggest that Tat-Ram13 holds promise as a novel therapeutic agent for targeting apoptosis-resistant cancers, offering a potential strategy for treating refractory hematopoietic malignancies.

5. EXPERIMENTAL SECTION

5.1. Chemicals and Reagents. Fmoc-protected amino acids, Wang PEG resin, and coupling reagents were purchased from Watanabe Chemical Co. (Hiroshima, Japan) or Peptide Institute Inc. (Osaka, Japan). The fluorescent dye 5(6)-carboxy-tetramethyl rhodamine, etoposide, EIPA, FITC-labeled 70 kDa dextran, and Hoechst 33342 were purchased from Merck Millipore (Burlington, MA). Primary antibodies were obtained from Cell Signaling Technology (CST) (Danvers, MA).

5.2. Cell Culture. All tumor cell lines and primary human peripheral blood mononuclear cells (PBMCs) listed in Table S1 were obtained from commercial sources and used in the study. The cells were maintained in a complete medium (RPMI-1640 supplemented with 10% fetal calf serum, 10 U/mL penicillin G, and 10 μg/mL streptomycin) in a 5% CO_2 atmosphere.

5.3. Peptide Synthesis. All peptides were synthesized in-house by the standard Fmoc solid-phase strategy using Initiator Alstra peptide synthesizer (Biotage, Uppsala, Sweden) or PSSM-8 System (Shimadzu, Kyoto, Japan). The peptides were cleaved from Wang PEG resin with a cleavage reagent consisting of trifluoroacetic acid (TFA)/triisopropylsilane/phenol/water (95/2/2/1). After cleavage, the peptides were precipitated with ice-cold diethyl ether. Therefore, the crude peptides were purified to >95% purity using reversed-phase HPLC (RP-HPLC) on C18 (250 × 21.2 mm) column (BGB Analytik AG, Boeckten, Switzerland) using a gradient system of 0.1% TFA in water as solvent A and 50% acetonitrile/0.1% TFA mixture as solvent B at a flow rate of 4 mL/min with UV detection at 220 nm. Peptide purity was determined by analytical RP-HPLC using a C18 (250 × 4.6 mm) column (Shiseido, Tokyo, Japan) with 0.1% TFA solution as solvent A and 90% acetonitrile/0.1% TFA as solvent B in a gradient solvent system with a flow rate of 1 mL/min. The molecular mass of the peptides was measured by AutoFlex II MALDI-TOF MS (Bruker Daltonics, Billerica, MA). The information in Table S2 and Figure S1 provides details about the purified peptides, including their assigned names, sequences, molecular masses, purities, and chromatographic spectra for each peptide.

5.4. Cytotoxicity Assay. Cells (5×10^4 cells/100 μL) in complete medium were seeded in a 96-well plate and then incubated with various concentrations of each peptide or etoposide in a CO_2 incubator for the indicated time. Cytotoxicity was assessed by measuring the absorbance at 450 nm with a microplate reader for 1−2 h after adding WST-8 reagent (Dojindo, Kumamoto, Japan) according to the manufacturer's guidelines. Cell viability of 100% was calculated by adding Hank's balanced salt solution (HBBS) as a control. For apoptosis inhibition assay, cells were pretreated with 50 μM z-VAD-fmk, a pan-caspase inhibitor, for 45 min and then added with 30 and 60 μM of Tat-Ram13 or etoposide for 24 h for 37 °C. Plasma membrane integrity was assessed based on LDH leakage from cells into the culture medium. The LDH amount was measured by assessing absorbance at 560 nm

https://doi.org/10.1021/acsomega.4c08955
ACS Omega 2024, 9, 49925−49934

using the LDH-Cytotoxic Test Wako (Wako, Osaka, Japan). 100% LDH leakage was determined in 0.2% (w/v) Tween 20.

5.5. Quantitative PCR Analysis. Human HPB-ALL cells in a complete medium were incubated with either a peptide, or DAPT for 16 h at 37 °C. Total RNA was extracted using the RNeasy Mini Kit (Qiagen, Hilden, Germany) and then converted to cDNA. The RNA was mixed with TB Green Premix Ex *Taq*II (Takara, Tokyo, Japan) and specific primers for *HES1, c-MYC, NOTCH1*, and the internal control *18S rRNA* (primer sets are listed in Table S3). PCR was performed using a StepOnePlus Real-Time PCR system (Thermo Fisher Scientific, Waltham, MA). The Ct values were normalized to *18S rRNA* using the ΔCt method, with the untreated group set as 1.0. Relative gene expression was then compared between the groups.

5.6. Fluorescence Microscopic Analysis. Cells (5×10^5 cells/well) were seeded in a 4-well glass bottom dish. The cells were incubated with or without 100 μM Tat-Ram13 or 30 μM etoposide for the indicated time. After treatment, the cells were incubated with Hoechst 33342 for 10 min. For observing macropinocytosis, the cells were preincubated with or without EIPA for 90 min and then 3 μM Tamra-Tat-Ram13 was added for 30 min. For the mitochondrial membrane potential assay, cells were incubated with 40 or 80 μM of Tat-Ram13 for 2 h at 37 °C and added with JC-1 assay reagent (Cayman Chemical, Ann Arbor, MI) for 10 min. The fluorescent images were observed using an FSX100 fluorescence microscope (Olympus, Tokyo, Japan) or Eclipse Ti2 confocal microscope (Nikon, Tokyo, Japan).

5.7. Measurement of Macropinocytic Activity. Cells seeded in a 6-well plate were incubated with 1 mg/mL of fluorescent-labeled FITC-70 kDa dextran in a complete medium for 30 min at 37 °C and then subjected to flow cytometric analysis using Accuri C6 Plus Flow Cytometer (B.D. Life Science, Franklin Lakes, NJ). The macropinocytic index, representing the degree of macropinocytosis, was quantified through flow cytometric analysis.

5.8. Western Blot Analysis. Cells (1×10^6) seeded in a 6-well plate were treated with 100 μM of Tat-Ram13 or etoposide in a CO_2 incubator for the indicated time. Cells were washed with ice-cold PBS and lysed in the RIPA buffer (Fujifilm, Tokyo, Japan) containing protease inhibitor cocktail Set I (Fujifilm). Cell lysates (25 μg) were separated on an SDS-polyacrylamide gel and electroblotted to a polyvinylidene difluoride membrane. The blots were blocked with 5% skim milk in PBS-Tween 20 (0.1%) for 30 min and probed overnight at 4 °C with the following 1:1000 diluted primary antibodies: caspase-3 (CST #9662), cleaved caspase-3 (Asp175) (CST #9664), PARP-1 (CST #9542), HMGB1 (CST #3935) and 1:10,000 diluted anti-β-actin antibody (PM053−7; Medical & Biological Lab., Tokyo, Japan). Then, the membranes were incubated with horseradish peroxidase (HRP)-conjugated secondary antibodies for 1 h at 4 °C, and protein bands were detected by the ImageQuant LAS400 image analyzer (G.E. HealthCare, Chicago, IL) with the Luminata Crescendo Western HRP substrate (Merck Millipore).

5.9. Hemolysis. The effect of the Tat-Ram13 peptide on mouse red blood cells was evaluated using a hemolysis assay as described. Fresh heparin-treated peripheral blood was collected from ddY mice (Japan SLC, Shizuoka, Japan) and centrifuged at 1000*g* for 5 min to prepare red blood cells as a 4% cell suspension in PBS. Subsequently, 50 μL of cells were incubated with various concentrations of Tat-Ram13 for 1 h at room temperature in a 96-well plate. After centrifugation, the absorbance of the supernatant was measured at 450 nm. Values of 100% hemolysis were obtained in the presence of 2%(w/v) Tween 20. Animal experimental procedures were performed according to guidelines for the Institutional Animal Care and Use Committee of Sojo University.

5.10. Statistical Analysis. Statistical analyses were conducted using GraphPad Prism 10.3.0 software or Microsoft Excel. All data are presented as means ± standard deviation (SD). Paired Student's *t*-test was used to compare paired data. A P value of less than 0.05 was considered statistically significant, with the following symbolic meanings: NS ($P > 0.05$), * ($P < 0.05$), ** ($P < 0.01$), *** ($P < 0.001$).

■ ASSOCIATED CONTENT

Supporting Information

The Supporting Information is available free of charge at https://pubs.acs.org/doi/10.1021/acsomega.4c08955.

Details and sources of the cell lines and primary cells, Details of synthesized peptides, chromatogram of purified peptides, primer sequences of human genes used for qPCR analysis, cytotoxicity and internalization of Tat-Ram13 in glioblastoma cells, Hemolytic activity of the peptides (PDF)

■ AUTHOR INFORMATION

Corresponding Author

Akihiko Kuniyasu − *Faculty of Pharmaceutical Sciences, Sojo University, Kumamoto 860-0082, Japan;* orcid.org/0000-0001-6104-5091; Email: kuniyasu@ph.sojo-u.ac.jp

Authors

Ryota Uchimura − *Faculty of Pharmaceutical Sciences, Sojo University, Kumamoto 860-0082, Japan*

Shinpei Nishimura − *Faculty of Pharmaceutical Sciences, Kumamoto University, Kumamoto 862-0973, Japan*

Mikako Ozaki − *Faculty of Pharmaceutical Sciences, Sojo University, Kumamoto 860-0082, Japan*

Manami Kurogi − *Faculty of Pharmaceutical Sciences, Kumamoto University, Kumamoto 862-0973, Japan*

Kohichi Kawahara − *Faculty of Pharmacy, Niigata University of Pharmacy and Applied Life Sciences, Niigata 956-0841, Japan*

Masaki Makise − *Faculty of Pharmaceutical Sciences, Sojo University, Kumamoto 860-0082, Japan*

Complete contact information is available at: https://pubs.acs.org/10.1021/acsomega.4c08955

Author Contributions

R.U. and S.N. contributed equally to this work. All authors conducted the experiments. R.U., S.N., and A.K. wrote the manuscript. All authors checked and approved the experimental results and the manuscript.

Notes

The authors declare no competing financial interest.

■ ACKNOWLEDGMENTS

This work was supported by JSPS KAKENHI grant nos. JP21K07206 and JP24K10465 (A.K.)

ABBREVIATIONS

CSL	CBF1/suppressor of hairless/Lag1
Fmoc	*N*-(9-fluorenyl)methoxycarbonyl
EIPA	5-(*N*-ethyl-*N*-isopropyl)amiloride
FITC	fluorescein isothiocyanate
HMGB1	high mobility group box 1
HRP	horseradish peroxidase
LDH	lactate dehydrogenase
MALDI-TOF-MS	matrix-assisted laser desorption/ionization-time-of-flight mass spectrometry
MAML	mastermind-like
NICD	notch receptor intracellular domain
NOTCH	notch receptor
PARP-1	poly(ADP-ribose)polymerase-1
PBS	phosphate-buffered saline
PI3K	phosphoinositide 3-kinase
PTEN	phosphatase and tensin homologue deleted from chromosome 10
RAM	RBP-jκ associated molecule
RIPA	radio immunoprecipitation assay
RP-HPLC	reverse-phase high-performance liquid chromatography
WST-8	water-soluble tetrazolium salt

REFERENCES

(1) Malard, F.; Mohty, M. Acute lymphoblastic leukaemia. *Lancet* **2020**, *395* (10230), 1146−1162.

(2) Belver, L.; Ferrando, A. The genetics and mechanisms of T cell acute lymphoblastic leukaemia. *Nat. Rev. Cancer* **2016**, *16* (8), 494−507.

(3) Cordo, V.; van der Zwet, J. C. G.; Cante-Barrett, K.; Pieters, R.; Meijerink, J. P. P. T-cell Acute Lymphoblastic Leukemia: A Roadmap to Targeted Therapies. *Blood Cancer Discov.* **2021**, *2* (1), 19−31.

(4) Shi, Q.; Xue, C.; Zeng, Y.; Yuan, X.; Chu, Q.; Jiang, S.; Wang, J.; Zhang, Y.; Zhu, D.; Li, L. Notch signaling pathway in cancer: from mechanistic insights to targeted therapies. *Signal Transduct. Target. Ther.* **2024**, *9* (1), 128.

(5) Tamura, K.; Taniguchi, Y.; Minoguchi, S.; Sakai, T.; Tun, T.; Furukawa, T.; Honjo, T. Physical interaction between a novel domain of the receptor Notch and the transcription factor RBP-J kappa/Su(H). *Curr. Biol.* **1995**, *5* (12), 1416−1423.

(6) Weng, A. P.; Ferrando, A. A.; Lee, W.; Morris, J. P. t.; Silverman, L. B.; Sanchez-Irizarry, C.; Blacklow, S. C.; Look, A. T.; Aster, J. C. Activating mutations of NOTCH1 in human T cell acute lymphoblastic leukemia. *Science* **2004**, *306* (5694), 269−271.

(7) Peng, F.; Liao, M.; Qin, R.; Zhu, S.; Peng, C.; Fu, L.; Chen, Y.; Han, B. Regulated cell death (RCD) in cancer: key pathways and targeted therapies. *Signal Transduct. Target. Ther.* **2022**, *7* (1), 286.

(8) Wang, X.; Hua, P.; He, C.; Chen, M. Non-apoptotic cell death-based cancer therapy: Molecular mechanism, pharmacological modulators, and nanomedicine. *Acta Pharm. Sin B* **2022**, *12* (9), 3567−3593.

(9) Wilson, J. J.; Kovall, R. A. Crystal structure of the CSL-Notch-Mastermind ternary complex bound to DNA. *Cell* **2006**, *124* (5), 985−996.

(10) Lubman, O. Y.; Ilagan, M. X.; Kopan, R.; Barrick, D. Quantitative dissection of the Notch:CSL interaction: insights into the Notch-mediated transcriptional switch. *J. Mol. Biol.* **2007**, *365* (3), 577−589.

(11) Lewis, H. D.; Leveridge, M.; Strack, P. R.; Haldon, C. D.; O'Neil, J.; Kim, H.; Madin, A.; Hannam, J. C.; Look, A. T.; Kohl, N.; et al. Apoptosis in T cell acute lymphoblastic leukemia cells after cell cycle arrest induced by pharmacological inhibition of notch signaling. *Chem. Biol.* **2007**, *14* (2), 209−219.

(12) Palomero, T.; Sulis, M. L.; Cortina, M.; Real, P. J.; Barnes, K.; Ciofani, M.; Caparros, E.; Buteau, J.; Brown, K.; Perkins, S. L.; et al. Mutational loss of PTEN induces resistance to NOTCH1 inhibition in T-cell leukemia. *Nat. Med.* **2007**, *13* (10), 1203−1210.

(13) Kannan, S.; Sutphin, R. M.; Hall, M. G.; Golfman, L. S.; Fang, W.; Nolo, R. M.; Akers, L. J.; Hammitt, R. A.; McMurray, J. S.; Kornblau, S. M.; et al. Notch activation inhibits AML growth and survival: a potential therapeutic approach. *J. Exp Med.* **2013**, *210* (2), 321−337.

(14) Kaplan, I. M.; Wadia, J. S.; Dowdy, S. F. Cationic TAT peptide transduction domain enters cells by macropinocytosis. *J. Controlled Release* **2005**, *102* (1), 247−253.

(15) Nakase, I.; Tadokoro, A.; Kawabata, N.; Takeuchi, T.; Katoh, H.; Hiramoto, K.; Negishi, M.; Nomizu, M.; Sugiura, Y.; Futaki, S. Interaction of arginine-rich peptides with membrane-associated proteoglycans is crucial for induction of actin organization and macropinocytosis. *Biochemistry* **2007**, *46* (2), 492−501.

(16) Nishimura, S.; Takahashi, S.; Kamikatahira, H.; Kuroki, Y.; Jaalouk, D. E.; O'Brien, S.; Koivunen, E.; Arap, W.; Pasqualini, R.; Nakayama, H.; et al. Combinatorial targeting of the macropinocytotic pathway in leukemia and lymphoma cells. *J. Biol. Chem.* **2008**, *283* (17), 11752−11762.

(17) Commisso, C.; Flinn, R. J.; Bar-Sagi, D. Determining the macropinocytic index of cells through a quantitative image-based assay. *Nat. Protoc* **2014**, *9* (1), 182−192.

(18) Stow, J. L.; Hung, Y.; Wall, A. A. Macropinocytosis: Insights from immunology and cancer. *Curr. Opin Cell Biol.* **2020**, *65*, 131−140.

(19) Rainero, E. Macropinocytosis at the crossroad between nutrient scavenging and metabolism in cancer. *Curr. Opin Cell Biol.* **2024**, *88*, No. 102359.

(20) Kim, S. M.; Nguyen, T. T.; Ravi, A.; Kubiniok, P.; Finicle, B. T.; Jayashankar, V.; Malacrida, L.; Hou, J.; Robertson, J.; Gao, D.; et al. PTEN Deficiency and AMPK Activation Promote Nutrient Scavenging and Anabolism in Prostate Cancer Cells. *Cancer Discov* **2018**, *8* (7), 866−883.

(21) Redelman-Sidi, G.; Iyer, G.; Solit, D. B.; Glickman, M. S. Oncogenic activation of Pak1-dependent pathway of macropinocytosis determines BCG entry into bladder cancer cells. *Cancer Res.* **2013**, *73* (3), 1156−1167.

(22) Chazotte, B. Labeling mitochondria with JC-1. *Cold Spring Harb. Protoc.* **2011**, *2011* (9), pdb.prot065490.

(23) Xu, Y.; Zhang, E.; Wei, L.; Dai, Z.; Chen, S.; Zhou, S.; Huang, Y. NINJ1: A new player in multiple sclerosis pathogenesis and potential therapeutic target. *Int. Immunopharmacol* **2024**, *141*, No. 113021.

(24) Jayashankar, V.; Edinger, A. L. Macropinocytosis confers resistance to therapies targeting cancer anabolism. *Nat. Commun.* **2020**, *11* (1), 1121.

(25) Moellering, R. E.; Cornejo, M.; Davis, T. N.; Del Bianco, C.; Aster, J. C.; Blacklow, S. C.; Kung, A. L.; Gilliland, D. G.; Verdine, G. L.; Bradner, J. E. Direct inhibition of the NOTCH transcription factor complex. *Nature* **2009**, *462* (7270), 182−188.

(26) Kayagaki, N.; Webster, J. D.; Newton, K. Control of Cell Death in Health and Disease. *Annu. Rev. Pathol* **2024**, *19*, 157−180.

(27) Tong, X.; Tang, R.; Xiao, M.; Xu, J.; Wang, W.; Zhang, B.; Liu, J.; Yu, X.; Shi, S. Targeting cell death pathways for cancer therapy: recent developments in necroptosis, pyroptosis, ferroptosis, and cuproptosis research. *J. Hematol. Oncol.* **2022**, *15* (1), 174.

(28) Chen, Z.; Wang, W.; Abdul Razak, S. R.; Han, T.; Ahmad, N. H.; Li, X. Ferroptosis as a potential target for cancer therapy. *Cell Death Dis.* **2023**, *14* (7), 460.

(29) Ashoub, M. H.; Razavi, R.; Heydaryan, K.; Salavati-Niasari, M.; Amiri, M. Targeting ferroptosis for leukemia therapy: exploring novel strategies from its mechanisms and role in leukemia based on nanotechnology. *Eur. J. Med. Res.* **2024**, *29* (1), 224.

(30) Zhou, H.; Forveille, S.; Sauvat, A.; Yamazaki, T.; Senovilla, L.; Ma, Y.; Liu, P.; Yang, H.; Bezu, L.; Muller, K.; et al. The oncolytic peptide LTX-315 triggers immunogenic cell death. *Cell Death Dis* **2016**, *7* (3), No. e2134.

https://doi.org/10.1021/acsomega.4c08955
ACS Omega 2024, 9, 49925−49934

(31) Akonnor, A.; Makise, M.; Kuniyasu, A. CXCR4-Targeted Necrosis-Inducing Peptidomimetic for Treating Breast Cancer. *ACS Omega* **2023**, *8* (27), 24467−24476.
(32) Furukawa, N.; Yang, W.; Chao, A. R.; Patil, A.; Mirando, A. C.; Pandey, N. B.; Popel, A. S. Chemokine-derived oncolytic peptide induces immunogenic cancer cell death and significantly suppresses tumor growth. *Cell Death Discov.* **2024**, *10* (1), 161.

https://doi.org/10.1021/acsomega.4c08955
ACS Omega 2024, 9, 49925−49934